

Modular Design and Modeling of an Upper Limb Exoskeleton

Javier Garrido, Wen Yu, Alberto Soria

Abstract—In this paper, we use modular design method to construct a 4-DoF (Degrees Of Freedom) upper limb exoskeleton. The structure is very simple, and is easy to be modified. Articulation of the exoskeleton is achieved four revolute joints: three for the shoulder and one for the elbow. Static and dynamic models of this exoskeleton are proposed. Experiments and analysis of the exoskeleton robot are carried out to evaluate the effectiveness of the design.

I. INTRODUCTION

The exoskeleton robot is worn by the human operator as a device. Its joints and links correspond to those of the human body. The same system operated in different modes can be used for three fundamental applications: device for teleoperation [32], human-amplifier [10], and physical therapy modality as part of the rehabilitation [36]. A wide variety of exoskeleton systems both for upper limbs [29] and lower limbs [16] with various human-machine interfaces have been developed. The first generation man-amplifier exoskeleton, known as Hardiman [25], used hydraulically powered articulating frame worn by an operator. The second generation of exoskeletons utilized the direct contact forces (measured by force sensors) between the human and the machine as the main command signals to the exoskeleton. The operator is in full physical contact with the exoskeleton throughout its manipulation [16]. The third generation of exoskeletons is defined by at higher levels of the human physiological (neurological) system hierarchy, such as electromyogram sensor [11][30].

Korein [17] is one of the first to study 7 degree-of-freedom (DoF) model for the human arm. Since then, many other researches have used it to study redundant robots [9] and upper limb exoskeletons [29], which neglects translational and rotational motion of the scapula and clavicle. Otherwise 9 DoF [8] and 11 DoF [24] models of the arm are needed. The 7 DoF arm model give a good combination of motion accuracy while reducing the model complexity to a manageable level. If we only consider motions of the shoulder and the elbow, the human arm has 4 DoF. This 4 DoF includes most of human arm motions. There are many 4 DoF exoskeleton robots [26]. The actuators of these exoskeletons include electric motors [28], pneumatic muscles [35], and hydraulic actuators [21]. The power transmission methods are gear drive [20], cable drive [29], and linkage mechanism.

Javier Garrido, Wen Yu and Alberto Soria are with Department of Automatic Control, CINVESTAV-IPN, Mexico City, Mexico. email:yuw@ctrl.cinvestav.mx

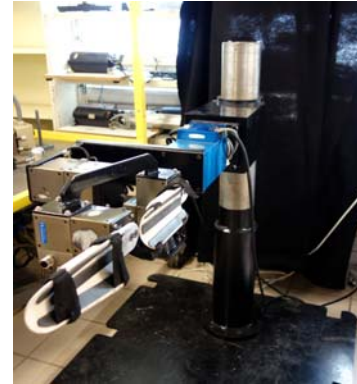


Fig. 1. CINVESRobot-1: 4 DoF upper limb exoskeleton

Although great progress has been made in a century-long effort to design and implement robotic exoskeletons, many design challenges continue to limit the performance of the system. The main problem is the design of the exoskeleton is complex to cope with human arm. In this paper we use the modular design concept. We use the PowerCube [33] motors as the basic elements for the joints of the exoskeleton. All joint modules are integrated using the universal communication interfaces CAN. Each joint has its own computer control system. The joint modules are fitted with a standardized interface for mechanism and control. So the design process is more simple and easy than the other exoskeletons [14].

The kinematics and dynamics of the human arm during activities of daily living are studied in part to determine the engineering specifications for the exoskeleton design. The model for the exoskeleton include forward kinematic, inverse kinematic, and dynamic model. The kinematics are used to calculate the relation between the joint angles and the arm position, while the dynamic model is applied to design controllers.

In this paper, we use PowerCube motors to design a 4-DoF upper limb exoskeleton, which is mounted on the ground. This allows both height and distance adjustment between the arms, see Fig1. Articulation of the exoskeleton is four single axis: three for the shoulder and one for the elbow. Static and dynamic models of this exoskeleton are proposed. Experiments and analysis of the exoskeleton robot are carried out.

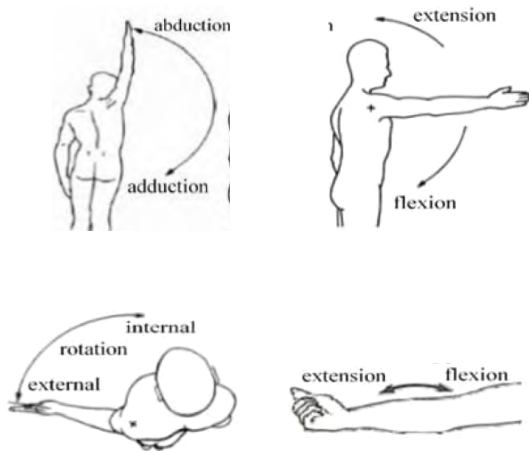


Fig. 2. Four basic motions of human arm

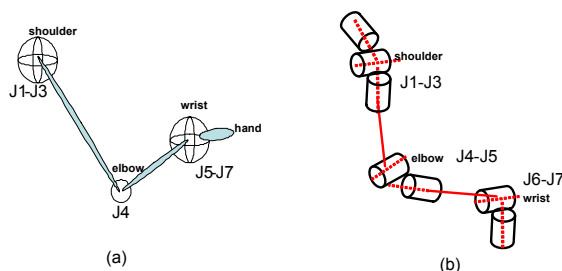


Fig. 3. Human arm rotations

II. A SIMPLE UPPER LIMB EXOSKELETON

A. Human Arm Model

The upper limb is composed of segments linked by articulations with multiple degrees of freedom. It is a complex structure that is made up of both ridged bone and soft tissue. This soft tissue moves and slides relative to the bone during movements and interactions with the environment. Additionally, muscle contractions cause changes to their shape and the overall stiffness of the arm. Although much of the complexity of the soft tissue is difficult to model, the overall arm movement can be represented by a much simpler model composed of rigid links connected by joints.

Three rigid segments, consisting of the upper arm, lower arm and hand connected by frictionless joints make up the simplified model of the human arm. Placing a reference frame at the shoulder, the upper arm and torso are rigidly attached by a ball and socket joint. This joint is responsible for three shoulder motions: abduction-adduction, flexion-extension and internal-external rotations. The connection between the upper and lower arm segments can be regarded as a single rotational joint at the elbow, see Fig.2. These motions can be regarded as several joint rotations as in Fig.3.



Fig. 4. Standard rotary module: PowerCube

In order to simplify the design process, we consider the case of Fig.3 (a), i.e., the elbow only has flexion-extension rotation, the lower arm and hand are connected by a spherical joint resulting in three wrist motions: pronation-supination, flexion-extension, and radial-ulnar deviation. In this paper we do not consider the wrist motion. So the arm has 4 DoF. The range of motion of the arm is shown in Table 1.

Table 1. Human arm performance

	abduction adduction	flexion extension	internal external	elbow
Range of motion	0:180	-45:180	-60:100	0:150
Daily living	0:80	-20:30	-30:40	20:80

B. Design of Upper Limb Exoskeleton

The fundamental principle in designing the exoskeleton joints is to align the rotational axis of the exoskeleton with the anatomical rotations axes. If more than one axis is at a particular anatomical joint (e.g. shoulder and wrist) the exoskeleton joints emulate the anatomical joint interaction at the center of the anatomical joint. Consistent with other work, the glenohumeral (G-H) [13] joint is modelled as a spherical joint composed of three intersecting axes. The elbow modelled by a single axis orthogonal to the third shoulder axis, with a joint stop to prevent hyperextension. Exoskeleton pron-sup takes place between the elbow and the wrist as it does in the physiological mechanism.

We use the PowerCube unit as standard rotary module, see Fig.4. It has brushless EC motors and a harmonic drive transmission. It uses single-cable technology to simply integrate the existing control concepts. The cubic geometry makes the system extremely adaptable for modular solutions. The joint Configuration and DoF selection are shown in Fig.5.

A result of representing the ball and socket joint of the shoulder, there are three intersecting joints. This spherical

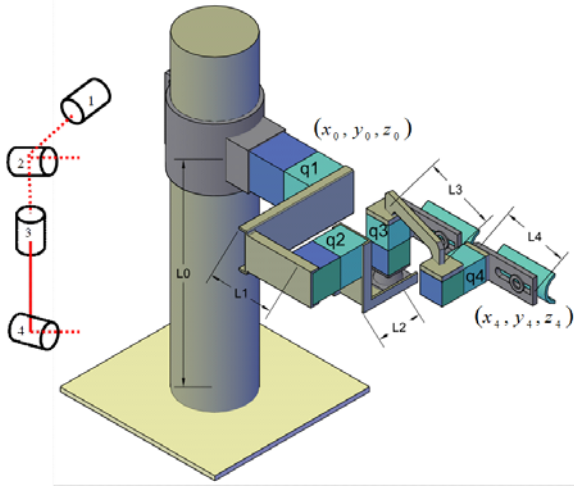


Fig. 5. Joint Configuration and DoF selection

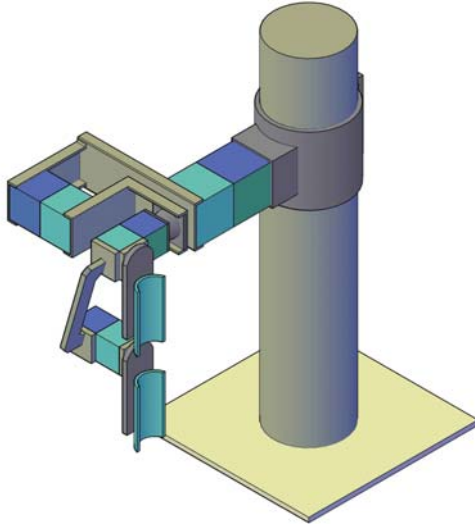


Fig. 6. Singularity in z_1 and z_3

approximation may introduce singularity when two joint axes are collinear, see Fig.6, z_1 and z_3 are not linearly dependent. A singularity is a device configuration where a DoF is lost or compromised as a result of the alignment of two rotational axes. The existence or nonexistence of singularity will depend entirely on the desired reachable workspace. Spherical workspaces equal to or larger than a hemisphere will always contain singular positions. The challenge is to place the singularity in an unreachable, or near-unreachable location, such as the edge of the workspace.

The servo positioning module combines high precision and high torque, and have a very compact design. The high torques are achieved by the integrated harmonic drive gears with considerable reserves of acceleration and

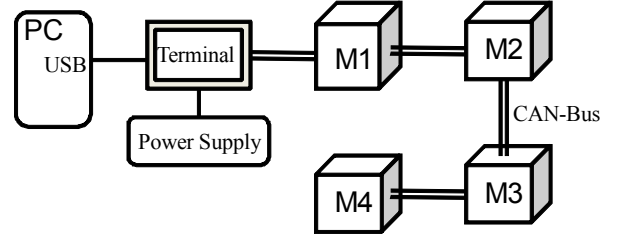


Fig. 7. Control system

deceleration, while the high-resolution encoder guarantees high precision. All of modules are connected by CAN bus (controller area network), see Fig.7. CAN allows microcontrollers and devices to communicate with each other without a host computer. The module can have a single CAN interface rather than analog and digital inputs to every device in the system. This decreases overall cost and weight of each joint. The new module can quickly be integrated into existing systems using the universal communication interfaces CAN.

The main difference between our design and the others is we apply modular design concept. This use the advantages of PowerCube motors, such as they are easily installed, each motor has its own control unit, the control network is CAN, etc.

III. DYNAMIC MODELING OF THE EXOSKELETON

The 7-DOF model of the upper limb exoskeleton shown in Fig. 3 is composed of a 3-DOF shoulder (J1-J3), a 1-DOF elbow (J4) and a 3-DOF wrist (J5-J7). J1-J3 are responsible for shoulder flexion-extension, abduction adduction and internal-external rotation, J4 creates elbow flexion-extension, J5-J7 are responsible for wrist flexion-extension, pronation-supination and radial-ulnar deviation, see Fig. 2.

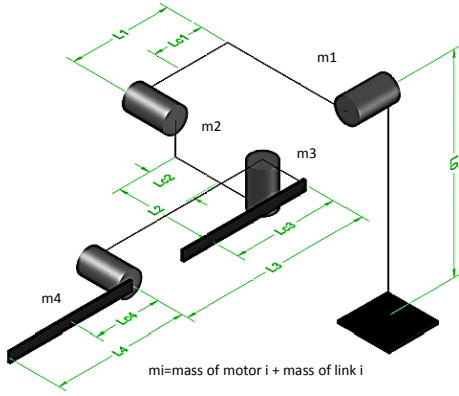
By D-H convention, we define each frame of the 4 DoF exoskeleton robots as in Fig. 3. The parameters of the frames of 4 DoF exoskeleton robot is shown in Table 3.

Table 3. Exoskeleton DH-parameters

Link	a_i	d_i	α_i	θ_i
1	0	l_1	$\frac{\pi}{2}$	q_1
2	0	l_2	$-\frac{\pi}{2}$	q_2
3	l_3	0	$\frac{\pi}{2}$	q_3
4	l_4	0	0	q_4

Many robot modeling tool can be used to calculate its dynamic by this his D-H convention. But this model is very complex, even for the homogeneous transformation matrix for the four joints are

$$T_1^i = A_1 \cdots A_i = \begin{bmatrix} R_0^i & o_0^i \\ 0 & 1 \end{bmatrix} \quad (1)$$



where $A_1 = \begin{bmatrix} c_1 & 0 & s_1 & 0 \\ s_1 & 0 & -c_1 & 0 \\ 0 & 1 & 0 & l_1 \\ 0 & 0 & 0 & 1 \end{bmatrix}$, $A_2 = \begin{bmatrix} c_2 & 0 & -s_2 & 0 \\ s_2 & 0 & c_2 & 0 \\ 0 & -1 & 0 & l_2 \\ 0 & 0 & 0 & 1 \end{bmatrix}$, $A_3 = \begin{bmatrix} c_3 & 0 & s_3 & l_3 c_3 \\ s_3 & 0 & -c_3 & l_3 s_3 \\ 0 & 1 & 0 & 0 \\ 0 & 0 & 0 & 1 \end{bmatrix}$, $A_4 = \begin{bmatrix} c_4 & -s_4 & 0 & l_4 c_4 \\ s_4 & c_4 & 0 & l_4 s_4 \\ 0 & 0 & 1 & 0 \\ 0 & 0 & 0 & 1 \end{bmatrix}$, $s_i = \sin(q_i)$, $c_i = \cos(q_i)$, $i = 1, \dots, 4$.

Forward Kinematic. The position of the end point of Joint 4 refer to the world frame (x_0, y_0, z_0) is

$$T_1^4 = A_1 A_2 A_3 A_4 = \begin{bmatrix} R_1^4 & o_1^4 \\ 0 & 1 \end{bmatrix}, \quad (x_4, y_4, z_4) = o_1^4 \quad (2)$$

o_1^4 is calculated from (1), the direction of the end point is R_1^4 .

Since T_1^4 is very complete, we also use geometric approach for calculating forward kinematic, see Fig. III,

$$\begin{aligned} x &= (l_3 \cos q_3 + l_4 \cos q_4) \sin q_1 \\ y &= (l_3 \cos q_3 + l_4 \cos q_4) \cos q_1 \cos q_2 \\ z &= (l_3 \cos q_3 + l_4 \cos q_4) \cos q_3 \sin q_2 + l_1 \end{aligned} \quad (3)$$

Dynamic Model. Fortunately, this upper limb exoskeleton is fixed on the human arm, (the behavior of the exoskeleton is the same as the human arm). We can regard J1, J2 and J3 in Fig. 2 as three spherical joints of human shoulder, see Fig. 3. The frame matrices of J1, J2, J3, and J4 are calculated from Table 4.

Dynamic model. The linear velocity is obtained by the chain rule for differentiation, the end-effector \dot{o}_0^n is

$$\dot{o}_0^n = \sum_{i=1}^n \frac{\partial o_0^n}{\partial q_i} \dot{q}_i = [J_{v_1} \dots J_{v_n}] \begin{bmatrix} \dot{q}_1 \\ \vdots \\ \dot{q}_n \end{bmatrix} \quad (4)$$

where $J_{v_i} = \frac{\partial o_0^n}{\partial q_i}$, $T_0^4 = \begin{bmatrix} R_0^4(q) & o_0^4 \\ 0 & 1 \end{bmatrix} =$

$T_0^{i-1} T_{i-1}^i T_i^4 = \begin{bmatrix} R_0^4 & R_0^i o_i^4 + R_0^{i-1} o_{i-1}^i + o_0^{i-1} \\ 0 & 1 \end{bmatrix}$, o_i is given by the first three elements of the fourth column of T_0^i . The dynamics of exoskeleton robots include translational kinetic, rotational kinetic, potential and friction. Translational kinetic energy is $K_T = \frac{1}{2} \dot{q}^T [\sum_{i=1}^n m_i J_{v_i}^T(q) J_{v_i}(q)] \dot{q}$. The rotational kinetic energy is $K_R = \frac{1}{2} \sum_{i=1}^n (\omega_0^i)^T I_i \omega_0^i = \frac{1}{2} \dot{q}^T [\sum_{i=1}^n J_{\omega_i}^T I_i J_{\omega_i}] \dot{q}$.

The potential energy of the manipulator is just the sum of those of the four links. For each link, the potential energy is just its mass multiplied by the gravitational acceleration and the height of its center of mass we see

$$\begin{aligned} V_1 &= 0 \\ V_2 &= -g l_c m_2 c_1 \\ V_3 &= g m_3 (l_{c3} c_1 s_3 - l_c c_1 + l_c c_2 c_3 s_1) \\ V_4 &= g m_4 (-c_1 l_2 + c_1 l_3 s_3 + c_2 c_3 l_3 s_1 + c_1 c_4 l_4 s_3) \\ &\quad - g m_4 (l_4 s_1 s_2 s_4 + c_2 c_3 c_4 l_4 s_1) \\ V &= V_1 + V_2 + V_3 + V_4 \end{aligned} \quad (5)$$

The dynamics of exoskeleton robots are derived from Euler-Lagrange equation

$$\frac{d}{dt} \frac{\partial L}{\partial \dot{q}} - \frac{\partial L}{\partial q} = \tau, \quad L = K - V, \quad K = K_T + K_R \quad (6)$$

The dynamic equation is

$$M(q) \ddot{q} + C(q, \dot{q}) \dot{q} + G(q) = \tau \quad (7)$$

where

$$\begin{aligned} M(q) &= D(q) \\ G(q) &= [\phi_1, \dots, \phi_4]^T, \quad \phi_i = \frac{\partial V}{\partial q_i} \\ C(q, \dot{q}) &= \{c_{kj}\}, \quad c_{kj} = \sum_{i=1}^n c_{ijk} \dot{q}_i, \quad k, j = 1 \dots n \end{aligned} \quad (8)$$

c_{ijk} is Christoffel symbols [34]

$$c_{ijk} = \frac{1}{2} \left(\frac{\partial d_{kj}}{\partial q_i} + \frac{\partial d_{ki}}{\partial q_j} - \frac{\partial d_{ij}}{\partial q_k} \right) \quad (9)$$

Usually, friction is the biggest problem for the control of robot manipulators. It is difficult, however, to prepare a perfect friction model for feedforward compensation because of the complexity of static and dynamic characteristics of friction such as the Saibeck effect, the Dahl effect, stick-slip motion, and so on. Furthermore, the amount of joint friction also changes because the moment of the gravity force acting on each joint varies when the configuration of the robot manipulator is changed. A friction model consists of negative viscous (including static friction), Coulomb, and viscous friction. A mathematical model which is similar to Tustin's model is

$$F(\dot{q}) = \begin{cases} F_s \exp \left[- \left(\frac{\dot{q}}{k} \right)^2 \right] & \dot{q} = 0 \\ F_k \operatorname{sgn}(\dot{q}) + F_v \dot{q} & \dot{q} \neq 0 \end{cases} \quad (10)$$

where F_s is the static friction, $k > 0$, F_k and F_v are the kinetic friction and the viscous friction parameters.

The final dynamic equation is

$$M(q)\ddot{q} + C(q, \dot{q})\dot{q} + G(q) + F(\dot{q}) = \tau \quad (11)$$

A. Actuators

The model of each servomotor can be divided into electrical and mechanical two subsystems. The electrical system is based on Kirchhoff's voltage law

$$U_i = L_i \dot{I}_i + R_i I_i + K_b \dot{\theta}_i \quad (12)$$

where U is input voltage, I_i is armature current, R_i and L_i are the resistance and inductance of the armature, K_b is back emf constant, $\dot{\theta}_i$ is angular velocity. Compared to $R_i I_i$ and $K_b \dot{\theta}_i$, the term $L_i \dot{I}_i$ is very small. In order to simplify the modeling and as most DC motor modeling methods, we neglected the term $L_i \dot{I}_i$. The mechanical subsystem is $\frac{1}{K_g} (J_i \ddot{\theta} + B_i \dot{\theta}) = \tau_i$, where K_g is gear ratio, J_i is the effective moment of inertia, B_i is viscous friction coefficient, τ_i is the torque produced at the motor shaft. The electrical and mechanical subsystems are coupled to each other through an algebraic torque equation $\tau_i = K_i I_i$, K_i is torque constant of the motor. Assume that there is no backlash or electric deformation in the gears, the work done by the load shaft equals to the work done by the motor shaft, $\tau = \frac{1}{K_g} \tau_i = \tau_i$, here τ is the torque on the frame of ball and beam system. So the DC motor model is

$$\frac{R_i J_i}{K_i K_g} \ddot{\theta} + \left(K_b + \frac{R_i B_i}{K_i K_g} \right) \dot{\theta}_i = U_i \quad (13)$$

IV. EXPERIMENT

Our upper limb exoskeleton is named CINVESRobot-1. The computer control platform is shown in Fig.7. The computer is an Intel Pentium4@2.4 GHz processor and 2G RAM. The operation software are Windows XP with Matlab 7.2 + WinCon. The real-time control programs also operated in Real-Time Target and. The communication interface is USB with CAN bus with DsPic . All of the controllers employ a sampling frequency of 500Hz. The joint modules are PowerCube PR 110-161, PR 90-161, and PR 70-161. The power supply for PR 110-161 is 48VDC and for the others 24 VDC. Joint-1 uses PR 110-161, Joint-2 uses PR 90-161, Joint-3 and Joint-4 use PR 70-161. The normal torques of them are 142Nm, 72Nm, and 23Nm. The weight of these modules are 5.6Kg, 3.4Kg, and 1.7Kg.

Several experiments are preformed to validate the model. Fig. 8 shows step response of the four joints. The controller of each joint module is standard PID. We can see that the position regulation of the joints works well.

The second test is to finish a rehabilitation task with CINVESRobot-1. The configuration is shown in Fig.9. We

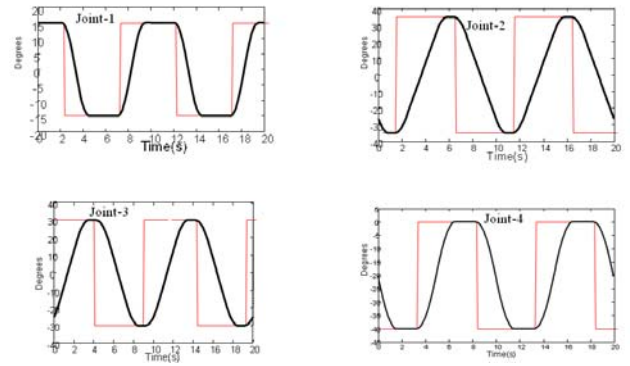


Fig. 8. Step response of each joint



Fig. 9. Rehabilitation test

use this experiment to check if the mechanical design is suitable for human arm, and if the safety requirements are satisfied. The safety steps includes the mechanical, electrical, and software designs. In the mechanical part has a physical stops prevent segments in the joints. The electrical part is added an emergency shutoff button to terminate motor motion. The most easy method is to use software to monitor power transmission integrity to limit motor currents, i.e., motor torques. When the motor moves near to the limits, a brake command is send to this motor, via software is selected maxim and minimum range of degree for the movements for each one.

Another advantages of this design is that the modular architecture is easy to be modified and increased according to the needs of rehabilitation. The industrial protocol CAN assures control and measurement signals reach their destination correctly. The control types are: position, torque and speed. These allow different types of platform for rehabilitation.

V. CONCLUSIONS

In this paper, a simple 4-DoF upper limb exoskeleton is designed with the modular technique. The system is very compact. This also allows easy modification. Articulation of the exoskeleton has four joints: three for the shoulder and one for the elbow. Static and dynamic models of this exoskeleton are proposed. Experiments on each motor and rehabilitation are proposed to test the effectiveness of our design.

The human shoulder is anatomically complex, Its center of rotation changes with movements. It is difficult for the robot exoskeleton to generate this movement, because the rotation center of the robot moves. In the future, we will consider passive drives to solve this problem.

REFERENCES

- [1] S. J. Ball, I. E. Brown, and S. H. Scott, "MEDARM: A rehabilitation robot with 5DOF at the shoulder complex," in Proc. IEEE/ASME Int. Conf. on Advanced Intell. Mechatronics, Zurich, Switzerland, 2007, pp. 1-6.
- [2] C. Carignan, M. Liszka, and S. Roderick, "Design of an Arm Exoskeleton with Scapula Motion for Shoulder Rehabilitation," in Proc. Int. Conf. on Advanced Robotics, Seattle, USA, 2005, pp. 524-531.
- [3] S. Calinon and A. Billard, "Stochastic gesture production and recognition model for a humanoid robot, IEEE/RSJ International Conference on Intelligent Robots and Systems (IROS 2005), 2769-2774, 2005.
- [4] R.M. Murray, Zexiang Li, and S. Shankar Sastry. *A Mathematical Introduction to Robotic Manipulation*. CRC Press, 1994.
- [5] R. S. Mosher, Force reflecting electrohydraulic servo manipulator, *Electro-Tech*. 138 (1960).
- [6] P. Rabischong, Robotics for the handicapped, in Proc. IFAC Control Aspects of Prosthetics and Orthotics (IFAC), Columbus, OH (May 1982), pp. 163-167.
- [7] H. Kazerooni and T. J. Snyder, Case study on haptic devices: Human-induced instability in powered hand controllers, *J. Guid. Contr. Dynam.* 18(1) (1995) 108-113.
- [8] P. Culmer, A. Jackson, M.C. Levesley, J. Savage, R.Richardson, J.A.Cozens, and B.B Bhakta, An admittance control scheme for a robotic upper-limb stroke rehabilitation system, *27th Annual Conference on Engineering in Medicine and Biology*, 5081-5084, 2005
- [9] J.J. Craig. *Introduction to Robotic Mechanics and Control*, Prentice Hall, Upper Saddle River, 3rd edition, 2005.
- [10] A.M. Dollar and H.Herr, Lower Extremity Exoskeletons and Active Orthoses: Challenges and State-of-the-Art, *IEEE Transactions on Robotics*, Volume 24, No. 1, pp. 1-15, August 2008
- [11] C.Ettore, J.Rosen, J.C. Perry, S.Burns, Myoprocessor for Neural Controlled Powered Exoskeleton Arm, *IEEE Transactions on Biomedical Engineering*, pp. 2387-2396, Vol. 53, No. 11, November 2006
- [12] A. Frisoli, L. Borelli, A. Montagner, S. Marcheschi, C. Procopio, F. Salsedo, M. Bergamasco, M. C. Carboncini, M. Tolaini, and B. Rossi, "Arm rehabilitation with a robotic exoskeleton in Virtual Reality," in Proc. of Int. Conf. on Rehabilitation Robotics, Noordwijk, The Netherlands, 2007, pp. 631-642.
- [13] B. A. Garner and M. G. Pandy. A kinematic model of the upper limb based on the visible human project (VHP) image dataset, *Computer Methods in Biomechanics and Biomedical Engineering*, Vol.2, 107-124, 1999
- [14] R.Gopura, K.Kiguchi, Mechanical Designs of Active Upper-Limb Exoskeleton Robots State-of-the-Art and Design Difficulties, *IEEE 11th International Conference on Rehabilitation Robotics*, 178-184, Kyoto, Japan, 2009
- [15] G. R. Johnson, D. A. Carus, G. Parrini, S. Scattareggia Marchese, and R. Valeggi, "The Design of a Five-Degree-of-Freedom Powered Orthosis for the Upper Limb," Proc. of the Institution of Mechanical Engineers Part H-J. Eng. in Medicine, vol. 215, no. 3, pp. 276-284, 2001
- [16] H.Kazerooni, R.Steger, The Berkeley lower extremity exoskeleton, *Journal of Dynamic Systems, Measurements, and Control-Transactions of the ASME*, Vol.128, 14-25, 2006
- [17] J.U. Korein, *A Geometric Investigation of Reach*, The MIT Press, 1985
- [18] H-S.Lo, S-Q.Xie, Exoskeleton robots for upper-limb rehabilitation: State of the art and future prospects, *Medical Engineering & Physics*, Vol.34, 261-268, 2012
- [19] L. Lucas, M. DiCicco, and Y. Matsuoka, "An EMG-Controlled Hand Exoskeleton for Natural Pinching," *J. Robotics and Mechatronics*, vol.16-B, no 5, 2004, pp. 482-488.
- [20] F. Martinez, etc., Design of a Five Actuated DoF Upper Limb Exoskeleton Oriented to Workplace Help, *2nd Biennial IEEE/RAS-EMBS International Conference on Biomedical Robotics and Biomechatronics*, 169-175, Scottsdale, USA, 2008
- [21] M. Mistry, P. Mohajerian, and S. Schaal, An Exoskeleton Robot for Human Arm Movement Study, *IEEE/RSJ Int. Conf. on Intell. Robots and Syst.*, 4071- 4076, Alberto, Canada, 2005.
- [22] M. Mihelj, T. Nef, and R. Riener, "ARMin-Toward a six DOF Upper Limb Rehabilitation Robot," in Proc. IEEE/RAS-EMBS Int. Conf. on Biomed. Robotics and Biomech., Pisa, Italy, 2006, pp. 1154-1159.
- [23] M. Mihelj, T. Nef and R. Riener, "ARMin II-7 DOF Rehabilitation Robot: Mechanism and Kinematics," in Proc. IEEE Int. Conf. on Robotics and Automat., Roma, Italy, 2007, pp. 4120-4125.
- [24] W.Maurel, *3D Modeling of the Human Upper Limb Including the Biomechanics of Joints, Muscles and Soft Tissues*, PhD thesis, Ecole Polytechnique Federale de Lausanne, 1998.
- [25] B. J. Makinson, Research and development prototype for machine augmentation of human strength and endurance, Hardiman I project, Report S-71-106, GE Company, Schenectady, New York, 1971.
- [26] S. Moubarak, M.T. Pham, T. Pajdla and T. Redarce, Design and Modeling of an Upper Extremity Exoskeleton, *11th International Congress on Medical Physics and Biomedical Engineering*, 476-482, Munich, Germany, 2009
- [27] T. Nef and R. Riener, "ARMin-Design of a Novel Arm Rehabilitation Robot," in Proc. Int. Conf. on Rehabil. Robotics, Chicago, USA, 2005, pp. 57-60.
- [28] T. Nef, M. Mihelj, G. Colombo, and R. Riener, ARMin-Robot for Rehabilitation of the Upper Extremities, *IEEE Int. Conf. on Robotics and Automat.*, 3152-3157, Orlando, USA, 2006.
- [29] C.Perry Joel, J.Rosen, S.Burns, Upper-Limb Powered Exoskeleton Design, *IEEE Transactions on Mechatronics*, Volume 12, No. 4, pp. 408-417, August 2007
- [30] J.Rosen, M.Brand, M.B.Fuchs, and M.Arcan, A myosignalbased powered exoskeleton system. *IEEE Transaction on Systems, Man, and Cybernetics - Part A: Systems and Humans*, 31(3):210-222, 2001.
- [31] J. C. Perry and J. Rosen, "Upper-Limb Powered Exoskeleton," Int. J. Humanoid Robotics, vol. 4, no. 3, 529-548, 2007.
- [32] J.L.Pons, *Wearable robots: biomechatronic exoskeletons*, San Francisco, CA: Wiley, 2007
- [33] <http://www.schunk-mechatronik.com/en/products/intelligent/rotary-actuator-prl.html>
- [34] Mark W.Spong and M.Vidyasagar, *Robot Dynamics and Control*, John Wiley & Sons Inc., Canada, 1989.
- [35] T. G. Sugar, etc., Design and Control of RUPERT: A Device for Robotic Upper Extremity Repetitive Therapy, *IEEE Trans. Neural Syst. Rehabil. Eng.*, Vol. 15, No. 3, 336-346, 2007
- [36] H.Van der Loos, D.J.Reinkensmeyer, Rehabilitation and health care robotics, *Handbook of Robotics*. New York, NY: Springer; p. 1223-1251, 2008.